

SPECTRAL DISTORTIONS OF THE COSMIC MICROWAVE BACKGROUND

FRED C. ADAMS,¹ KATHERINE FRESE, ² JANNA LEVIN, ² AND JONATHAN C. McDOWELL¹

Received 1988 December 30; accepted 1989 February 22

ABSTRACT

Motivated by recent experiments indicating that the spectrum of the cosmic microwave background deviates from a pure blackbody, we consider spectral distortions produced by cosmic dust. Our main result is that cosmic dust in conjunction with an injected radiation field (perhaps produced by an early generation of very massive stars) can explain the observed spectral distortions without violating existing cosmological constraints. In addition, we show that Compton γ -distortions can also explain the observed spectral shape, but the energetic requirements are more severe.

Subject headings: cosmic background radiation — cosmology — radiation mechanisms

I. INTRODUCTION

If the cosmic microwave background exhibits spectral distortions as reported by Matsumoto *et al.* (1988), then interesting modifications of the standard history of the universe in big bang cosmology are required. Here, we show that the observed distortions can be produced by the combination of cosmic dust grains and an energetic radiation field, perhaps generated by an early generation of very massive stars. In this case, large amounts of energy and dust must be injected into the universe at relatively high redshift ($20 \leq z \leq 50$). Although the energy and dust requirements are large, they are consistent with present cosmological constraints. In addition, we show that the observed spectral shape is also consistent with that produced by Compton γ -distortions.

The cosmic microwave background (CMB), originally discovered by Penzias and Wilson (1965), is an important probe of the universe since the epoch of last scattering of photons at the recombination redshift ($z_{\text{rec}} \simeq 10^3$ in the standard model). Prior to that time, the rate for Compton scattering of photons with electrons was large compared to the expansion rate of the universe and the universe was essentially opaque. Since that time, the background photons have not interacted and the CMB allows us to study conditions of the universe back to the recombination epoch. At present, the CMB is our only direct probe of physics between redshifts of about 5 – 10^3 .

Observations of the CMB have shown it to be a Planck spectrum with a temperature of ~ 2.74 K in the Rayleigh-Jeans (long wavelength) portion of the spectrum. However, a rocket flight in 1987 by the Nagoya-Berkeley collaboration (see Matsumoto *et al.* 1988) reported a spectral distortion of the CMB. They found an excess in the Wien part of the spectrum that corresponds to a 20% excess in energy density. (We find that if we fit a smooth curve through the observed data points, the total area under the curve corresponds to a 20% excess.) The three symbols in Figures 2–9 below at wavelengths 1160, 710, and $480 \mu\text{m}$ are their data points; the fourth symbol at $260 \mu\text{m}$ is an upper limit as it includes contributions from interstellar dust. An independent balloon-borne experiment (Bernstein *et al.* 1989) has shown that the spectral distortion observed in the first three channels of Matsumoto *et al.* must have an extragalactic origin. The excess peaks at the second point, $\lambda = 706$

μm , where the observed flux is ~ 1.7 times that expected from a Planck distribution with $T = 2.74$ K.

In this paper we show that cosmic dust provides a viable mechanism to explain the observed spectral distortion. In this model, the dust absorbs and reradiates photons from an energy source such as Population III stars. Models of this type (see Rowan-Robinson, Negroponte, and Silk 1979; Puget and Heyvaerts 1980; Wright 1981; Negroponte, Rowan-Robinson, and Silk 1981) have been considered previously to explain spectral distortions reported by an earlier generation of experiments (Woody and Richards 1981) and subsequently attributed to systematic effects. Related work has been done to study the plausibility of an early generation of massive stars (Negroponte 1986; Bond, Carr, and Hogan 1986; McDowell 1986). For the distortion observed recently (Matsumoto *et al.* 1988), Hayakawa *et al.* (1987) have considered heuristic dust models and Lacey and Field (1989) have considered energetic constraints. However, we perform detailed dust distortion calculations which actually solve the full radiative transfer problem with realistic opacities (see also Draine and Shapiro 1989) and then apply our results to the newly observed distortions. We also briefly consider the process of Comptonization, where hot electrons scatter photons up to higher energies (see, e.g., the review of Sunyaev and Zel'dovich 1980). We show that both mechanisms can produce the observed spectral shape, and we focus primarily on the dust scenario to present predictions from specific models. Both scenarios require a rather large modification of the standard picture of the universe between redshifts of 5 and 10^3 : the dust scenarios require the existence of significant amounts of dust and an energy source; the Comptonization scenarios need large amounts of energy to heat the electrons.

The paper is organized as follows. We first formulate the radiative transfer problem for dust distortions in § II and then specify the physical variables in § III. The results of our dust distortion models are presented in § IV and the effects of Compton scattering are considered in § V. We conclude with a discussion (§ VI) of our results and their astrophysical implications.

II. RADIATIVE TRANSFER IN AN EXPANDING UNIVERSE

Here we posit the existence of an energy source which gives rise to a flux of photons at a large redshift z_* . The energy source could, for example, be an early generation of stars.

¹ Harvard-Smithsonian Center for Astrophysics, Cambridge, MA 02138.

² Massachusetts Institute of Technology, Cambridge, MA 02139.

However, the details of the source spectrum are irrelevant as long as enough energy is deposited into the universe at optical or UV wavelengths. Cosmic dust, which is formed at a redshift z_D and is distributed homogeneously and isotropically, then absorbs and reradiates the radiation from the energy source.

Before the epoch z_D (we assume $z_D \leq z_*$), the radiation field of the universe consists of two components: the cosmic microwave background and the radiation field due to the sources. After dust is introduced, the radiation field evolves according to the equation of radiative transfer in an expanding universe. In the present context, at any given redshift z after z_D the equation of transfer has the formal solution (see e.g., Rowan-Robinson, Negroponte, and Silk 1979),

$$I_\nu(z) = B_\nu[T_{\text{CMB}}(z)] \exp[-\tau_\nu(z_D, z)] + S_\nu(z) \exp[-\tau_\nu(z_D, z)] + \int_z^{z_D} B_\nu \left[\frac{T_D(z')(1+z)}{(1+z')} \right] \exp[-\tau_\nu(z', z)] \frac{d\tau_\nu}{dz'} dz' , \quad (1)$$

where B_ν is the Planck function, $S_\nu(z)$ is the spectrum of the sources and where $\tau_\nu(z_D, z)$ is the optical depth of material between the epoch z_D and the epoch z and is given by

$$\tau_\nu(z_D, z) = \int_z^{z_D} \Omega_D \rho_C \kappa_\nu c \frac{dt}{dz'} dz' . \quad (2)$$

Notice that the opacity κ_ν is normalized relative to the total dust density $\Omega_D \rho_C$ and must be evaluated at the instantaneous frequency $\nu' = \nu(1+z)/(1+z)$ of the photon, where ν is the frequency at the redshift z . Since the opacity is an increasing function of frequency (except near the spectral features; see Fig. 1), the optical depth grows with redshift faster than predicted by the increase in column density alone. In the formal solution (1), the temperature distribution $T_D(z)$ of the dust is unknown and must be determined by the equation of radiative balance

$$\int_0^\infty B_\nu[T_D(z)] \kappa_\nu d\nu = \int_0^\infty I_\nu(z) \kappa_\nu d\nu , \quad (3)$$

where the left-hand side of the equation is the energy emitted by the dust and the right-hand side of the equation is the energy absorbed by the dust.

As indicated by equation (1), the radiation field can be separated into three distinct components: the (original) microwave background, the stellar (or other UV) radiation field, and the diffuse radiation field produced by dust emission. For the regime of parameter space applicable to the observed distortions, the universe must be optically thin to radiation at the peak of the CMB and must be optically thick to the stellar (or other UV) photons. Hence, the original microwave background photon distribution will be essentially unaffected by the presence of cosmic dust. On the other hand, essentially all of the stellar photons will be absorbed and re-emitted by the dust grains.

We solve the radiative transfer problem using the numerical code described in McDowell (1986). An outline of the numerical procedure is given in the appendix to this paper. The result of solving the coupled equations is a self-consistent temperature profile $T_D(z)$ for the dust and the spectrum of radiation I_ν at the present epoch. We examine the possibilities in parameter space and find that our options for matching the observed data points are in fact quite limited.

III. PARAMETERS OF THE THEORY

Before we can solve the set of equations (1)–(3) to find the resulting spectral distortions of the CMB, we must first specify the physical characteristics of the expanding universe, the unperturbed CMB, the injected radiation field, and the cosmic dust grains. Here we describe the parameters available for our specification and indicate the choices we have made for our standard model; later we explore deviations from these choices.

a) The Universe

The basic universe is described by the Hubble parameter H_0 and by the total energy density of the universe $\Omega_0 = \rho/\rho_C$ (where ρ_C is the critical density). We use $H_0 = 50 \text{ km s}^{-1} \text{ Mpc}^{-1}$ for our standard case and define $h_{50} \equiv H_0/(50 \text{ km s}^{-1} \text{ Mpc}^{-1})$. For the total density of the universe, we take $\Omega_0 = 1$, i.e., $\rho = \rho_C = 4.7 \times 10^{-30} h_{50}^2 \text{ g cm}^{-3}$.

Except for the spectral distortions being considered in this paper, the spectrum of the cosmic microwave background is

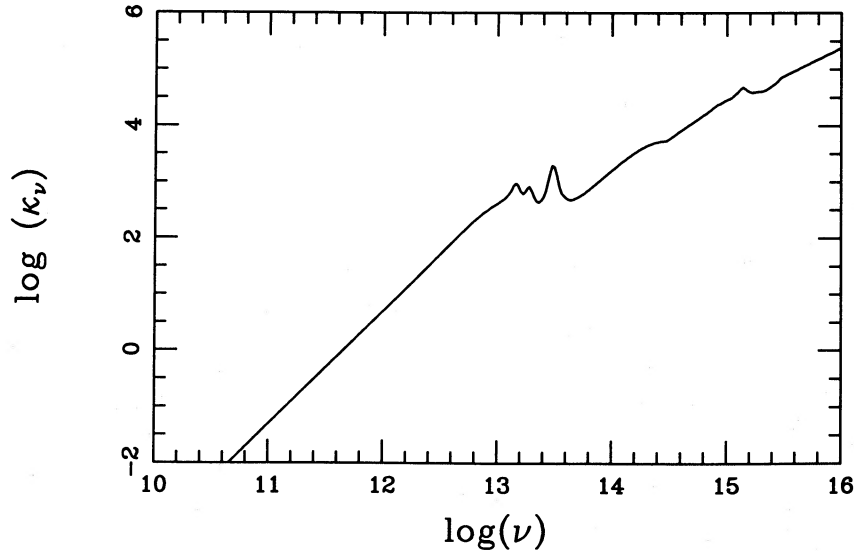


FIG. 1.—The interstellar extinction curve κ_ν . The frequency ν is given in hertz, the opacity κ_ν is given in $\text{cm}^2 \text{ g}^{-1}$. Notice the graphite feature in the ultraviolet region, the silicate features in the mid-infrared, and the $\kappa_\nu \propto \nu^2$ dependence at low frequencies.

well described by a blackbody of temperature T_0 . The value of T_0 is determined by experimental measurements on the long-wavelength side of the spectrum (for recent results, see Kogut *et al.* 1988; Johnson and Wilkinson 1987) and we adopt $T_0 = 2.74$ K for this present work.

b) Sources

We assume that energy sources (e.g., Population III stars) produce a homogeneous and isotropic radiation field S_v at a redshift z_* . In order to consider a specific case, we take our sources to be very massive objects (VMOs) of the type considered by Bond, Carr, and Arnett (1984). The source spectrum S_v then has the form of a blackbody $B_v(T_*)$, where the effective photospheric temperature is taken to be $T_* = 10^5$ K. As mentioned earlier, the results of our calculation are insensitive to the details of the spectrum S_v as long as enough energy ($\sim 20\%$ of CMB) is produced in reasonably short wavelength photons. Essentially all of these photons will get reprocessed by dust grains and their exact initial distribution will get washed out. Since all stellar photospheres are reasonably hot (they radiate optical or UV photons), these conditions will be met by any type of stellar object. We consider VMOs (i.e., stars with masses in the range $200 M_\odot \leq M_* \leq 10^5 M_\odot$) so that the sources collapse to black holes at the end of their lifetimes and do not pollute the universe with heavy elements (see Carr, Bond, and Arnett 1984).

Hence, the only relevant parameter of the sources is the total energy of the emitted radiation field. For a model in which the radiation is produced by VMOs, this total energy is determined by the total density of the sources Ω_* and by the efficiency ϵ of converting matter into radiation. We take the value $\epsilon = 4.1 \times 10^{-3}$ (see Bond, Carr, and Arnett 1984), which is approximately the maximum realistic efficiency that can be obtained for stellar objects (for a reference point, the corresponding efficiency of converting matter into energy for the Sun is $\epsilon \approx 7 \times 10^{-4}$). Larger net efficiencies could be obtained if we assumed more than one generation of VMOs, but doing so would result in an overabundance of heavy elements.

c) Dust Properties

In this model, we assume a homogeneous distribution of dust with a relative density Ω_D extending out to a dust formation redshift z_D . If the dust were not distributed homogeneously, (unobserved) anisotropies in the CMB could result (see Hogan and Bond 1988 for further discussion of this issue); in any case, inhomogeneities will not affect the spectral calculation. The amount of dust in the universe is constrained by QSO reddening and metallicity constraints to satisfy $\Omega_D < 10^{-4}$ (e.g., Wright 1981); we consider values in the range $10^{-6} - 10^{-4}$. Since the intrinsic spectra of low-redshift quasars show a scatter equivalent to a visual absorption of 1 mag, i.e., $A_V = 1$, (McDowell *et al.* 1989), an intergalactic optical depth of this amount to higher redshift quasars cannot be ruled out.

The dust opacity κ_v is assumed to have the same form as the dust opacity in the present-day interstellar medium of our galaxy (see Fig. 1). This dust is composed of both silicate and graphite grains. For high frequencies (i.e., $v \geq 5 \times 10^{14}$ Hz), the opacity has been fitted to the observed interstellar extinction curve (Savage and Mathis 1979) and has been linearly extrapolated ($\kappa_v \propto v$) for frequencies in the far UV where no data exist. At lower frequencies, the opacity is calculated by assuming that the grains are dielectric spheres with given

optical properties. The dielectric functions for graphites and silicates are specified by both theory (see Draine and Lee 1984) and laboratory experiments (see Adams and Shu 1986 and Shu, Adams, and Lizano 1987 for further details). Notice the silicate features at 10 and 20 μm , the graphite feature at 2200 Å, and the v^2 form of the opacity at long wavelengths.

Since the universe is assumed to be homogeneous and isotropic, only the absorptive portion of the extinction has been included in our calculations. Scattering of photons (i.e., changes of photon direction at constant energy) can be neglected since every photon scattered out of a given beam of radiation is replaced by a photon scattered into the beam.

In order to reduce the number of parameters, we will assume that the dust forms at the same epoch as the sources, i.e., $z_D = z_* \equiv z$. Since the optical depth of the dust must be (relatively) large for this scenario to work, we are in fact confined to deviate very little from this assumption. There is, however, a slight ambiguity in the physics, depending on whether z_D is precisely the same redshift as z_* or slightly later. If all of the source radiation is injected into the universe instantaneously and the dust is introduced shortly after the radiation injection (i.e., z_D is slightly less than z_*), then the dust is embedded in a UV radiation field of high-energy density. In this case, the initial dust temperature will be quite high. If, on the other hand, the sources radiate over a finite lifetime, and dust is present during the entire lifetime, then the UV radiation will be absorbed (and reradiated) as fast as it is produced; the dust temperature will only exceed the CMB radiation temperature initially by a small amount. After a brief initial phase, both scenarios will become the same and the dust temperature distribution will approach the simple analytic estimate $T_D(z) = T_{D0}(1+z)$ and we find $T_{D0} \approx 3$ K for all our models. For the two cases, the only difference in the resulting spectrum is that the high-frequency flux from dust *emission* (which appears at frequencies near channel 4 for the cases of interest) will be larger for the "instantaneous injection" scenario. In any event, the overall effect is not large, and we have used the finite lifetime scenario for the results presented in this paper. The value of the finite lifetime (we use $\tau \approx 1.7 \times 10^6$ yr) of the sources does not affect the results as long as τ is short compared to the age of the universe. The maximum dust temperature achieved in either scenario is a few hundred degrees, well below the temperature at which galactic dust melts (~ 1500 K).

d) Summary of Parameters

We now summarize our specification of the physical variables. We fix the parameters of the universe and the CMB at characteristic values determined through observations. The spectrum of the sources is unimportant and is taken to be a simple blackbody; the dust opacity has the form of present-day interstellar dust. Three parameters remain: the relative density of dust Ω_D , the relative density of Population III sources Ω_* , and the epoch of formation of stars and dust $z = z_D = z_*$. As shown below, two of these parameters, Ω_* and z , are related by energy considerations, and we are really left with only one parameter Ω_D at each redshift z .

e) Energy Considerations

As we show in the following section, for a given epoch of formation (in the range $20 \leq z \leq 50$), there are values of Ω_* and Ω_D that can produce the observed distortions. However, only for a more limited range of redshifts will the required values of Ω_D and Ω_* remain consistent with existing cosmo-

logical constraints. Here we illustrate the relation between the redshift of formation z and the density of sources Ω_* given by energy conservation.

The energy in the observed submillimeter excess is $\sim 20\%$ of the energy in the cosmic microwave background, i.e.,

$$\Omega_{\text{excess}} \approx 0.20\Omega_{\text{CMB}} \approx 2 \times 10^{-5},$$

since $\Omega_{\text{CMB}} = aT_0^4/\rho_C c^2 = 1.0 \times 10^{-4}$. The energy density of the radiation field produced by the sources is simply $\Omega_R(\text{emitted}) = \epsilon\Omega_*$ at the epoch of emission and is redshifted by a factor of $(1 + z_*)$ at the present epoch (recall that ϵ is the efficiency of converting matter into radiation). In order for the injected radiation field to be energetic enough to explain the observed excess, we require

$$\frac{\epsilon\Omega_*}{1 + z_*} \geq \Omega_{\text{excess}} \approx 2 \times 10^{-5}, \quad (4a)$$

where we have allowed for the possibility that not all of the source radiation will be processed into the observed excess. If we assume the most efficient energy conversion factor $\epsilon = 4.1 \times 10^{-3}$ (appropriate for VMOs—see Carr, Bond, and Arnett 1984), the energetic constraint becomes

$$\frac{\Omega_*}{1 + z_*} \geq 4.8 \times 10^{-3}. \quad (4b)$$

For various choices of formation redshift z , we list in Table 1 the minimum values of Ω_* that are required to explain the observed excess within the context of the VMO model. If the efficiency ϵ is lower or if a substantial amount of source radiation is not processed into submillimeter wavelengths the required values of Ω_* will be larger.

Since these very massive stars are likely to consist of baryonic matter, constraints on the total baryonic energy density Ω_b from big bang nucleosynthesis (BBN) can be used to constrain the allowed values of Ω_* and hence the allowed values of z . He⁴, He³, and deuterium abundances in the standard model of nucleosynthesis require $\Omega_b h_{50}^{-2} \leq 0.20$ (see Yang *et al.* 1984). Hence, in our models, $\Omega_* \leq 0.20$ and $z_* \leq 40$ (see Table 1). New lithium abundance estimates from Population II stars indicate stronger limits, i.e., $\Omega_b h_{50}^{-2} \leq 0.08$ (Kawano, Schramm, and Steigman 1988). However, these more stringent limits depend on the extrapolation of observed lithium abundances in Population II stars to the primordial abundance, an extrapolation that may break down, particularly in the VMO scenario considered here. Although most of the heavy elements produced by these stars must end up in remnant black holes, some of the heavy elements can be left behind to produce the Population II metallicity and perhaps even the cosmic dust. Nonstandard models of primordial nucleosynthesis, which

take into account inhomogeneities in the nucleon density that may arise at the quark/hadron transition, may even accommodate $\Omega_b = 1$ (e.g., see Fuller, Mathews, and Alcock 1987; Applegate, Hogan, and Scherrer 1987; Sale and Mathews 1986; Alcock, Fuller, and Mathews 1987). For this paper we restrict ourselves to models with $\Omega_b h_{50}^{-2} \leq 0.20$.

IV. RESULTS FOR DUST DISTORTIONS

For a given redshift of formation z , Ω_* is determined by the energy constraint of the previous section. We find that with the single remaining parameter, Ω_D , we can fit the observed spectrum for any z . In fact, we can obtain adequate agreement with the experimental data for a range of Ω_D values. In Figures 2–8, we show one particular sequence of models for the observed excess for redshifts in the range $20 \leq z \leq 50$. We plot the quantity $\Omega_v \equiv 4\pi v I_v / \rho_C c^3$, the fraction of the energy density of the universe in photons, as a function of frequency v . Note that the 10 μm silicate feature in the dust opacity appears as an emission feature (hence the bump in the spectrum in Figures 2–9, e.g., at $v \approx 8 \times 10^{11}$ Hz in Fig. 4).

The sequence of models presented above, parameterized by z and Ω_D , can be understood by the requirement that the total optical depth of the universe be within a given range. An analytic approximation to the optical depth integral in equation (2) implies that

$$\tau_v \propto \Omega_D (1 + z_D)^{n+3/2}, \quad (5)$$

where n is the spectral index of the dust opacity (here z_D is not necessarily the same as z_*). Since n corresponds to the average spectral index over the frequency range v to $(1 + z_D)v$, we can take $n = 1$ for photons with frequencies higher than the peak of the observed excess at the present epoch. Empirically we find that for formation redshifts in the range 35–50, we can fit the observed data using a sequence of models with a (roughly) constant optical depth at a given frequency (see Figs. 2–5 and Table 1), i.e., Ω_D varies with z_D according to equation (5). For formation redshifts in the range 20–30, we can fit the observed data using a sequence with a larger (but constant) optical depth (see Figs. 6–8 and Table 1). The entire sequence of models (Figs. 2–8) correspond to the lowest possible values of Ω_D that fit the data.

The transition from a large optical depth to a lower optical depth (as z_D increases) is due to the presence of the silicate features and to redshift effects. For formation redshifts in the range 25–30, the silicate feature appears in channel 4 (see Figs. 6 and 7). Hence, to avoid exceeding the upper limit in channel 4, the universe must be optically thick to the silicate feature. For formation redshifts $z_D \geq 35$, the silicate feature does not contribute to the flux in channel 4 and much lower optical depths (and Ω_D values) are allowed (see Table 1). For large formation redshifts ($z_D \geq 35$), a fairly wide range of Ω_D values result in adequate agreement with the observed spectrum; the Ω_D values used in Figures 2–5 are near the lower end of the allowed range. The strength of the silicate emission feature decreases with increasing Ω_D ; if subsequent observations show that no silicate feature is present, larger dust abundances (or lower relative abundances of silicates) may be necessary to fit the data.

Redshift effects also complicate the optical depth required by the models. For a given formation redshift z_D , most of the contribution to the optical depth occurs at the largest redshifts (see eq. [5]). Hence, most of the radiative transfer effects occur near z_D ; at epochs sufficiently later than z_D , the entire spectrum

TABLE 1
PARAMETERS FOR DUST
DISTORTION MODELS

z	Ω_*	Ω_D
20.....	0.100	2.0×10^{-4}
25.....	0.125	1.0×10^{-4}
30.....	0.150	7.0×10^{-5}
35.....	0.175	5.0×10^{-6}
40.....	0.200	2.0×10^{-6}
45.....	0.225	1.5×10^{-6}
50.....	0.250	1.0×10^{-6}

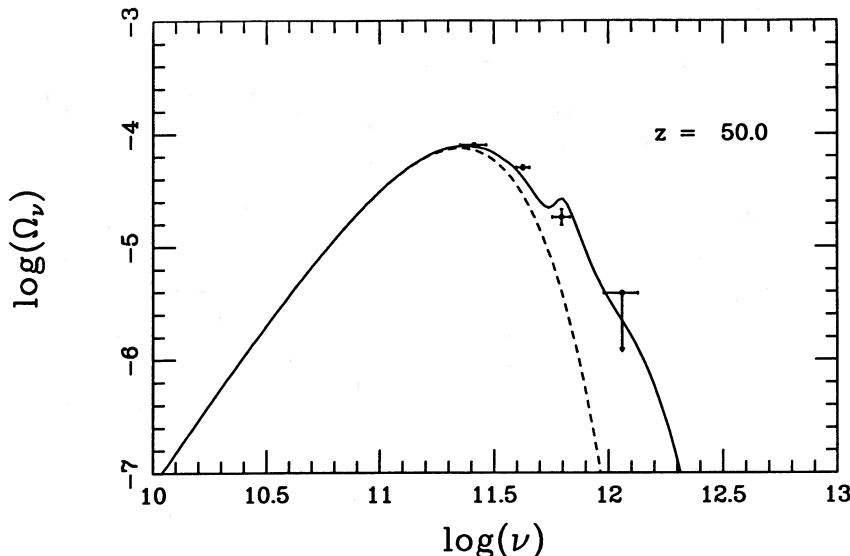


FIG. 2.—Dust distortion model at formation redshift $z = 50$. The original cosmic microwave background is shown as the dashed line; the total background is shown as a solid line and includes the contribution from a dust distortion model with $\Omega_* = 0.250$ and $\Omega_D = 1.0 \times 10^{-6}$. The flux is given in units of $\Omega_\nu \equiv 4\pi\nu I_\nu/\rho_C c^3$ (see text), and ν is in hertz. The symbols show the experimental data with error bars (in the vertical direction) and band widths (in the horizontal direction); the fourth point at $\nu \approx 1.1 \times 10^{12}$ Hz is an upper limit.

simply redshifts together (i.e., the spectrum moves to the left in Figures 2–8 with the same shape). For a given optical depth τ_ν of the universe, the spectra at the present epoch tend to become “redder” as the formation redshift z_D increases. Consequently, as z_D increases, smaller total optical depths are required to obtain the same (observed) spectral shape. The net result for our sequence of the complications discussed in the last two paragraphs is to produce the transition from a higher optical depth to a lower one as z_D increases.

For our sequence of models, the dust abundance becomes larger than the maximum allowed value $\Omega_D = 10^{-4}$ at a formation redshift of $z_D \approx 25$. For lower redshifts of dust formation, the required values of Ω_D increase roughly in accordance with equation (5); hence, for our standard set of parameters, the

dust formation epoch must occur at redshifts larger than $z_D \approx 25$. For larger redshifts of dust formation ($z_D > 25$), the required values of Ω_D decrease (see Table 1) and no conflict with the dust upper limit arises.

Thus, we have discovered a sequence of models which can be understood in terms of two physical quantities: the total energy of the injected radiation field and the total optical depth of the universe (see above). At high redshifts, energetic requirements constrain the redshift of star formation (e.g., for efficiency $\epsilon = 4.1 \times 10^{-3}$ and $\Omega_b \leq 0.20$, $z_* \leq 40$); at low redshifts, limits on the cosmic dust abundance imply $z_D \geq 25$. However, dust distortion models with any formation redshift in the range $25 \leq z \leq 40$ remain consistent with cosmological constraints.

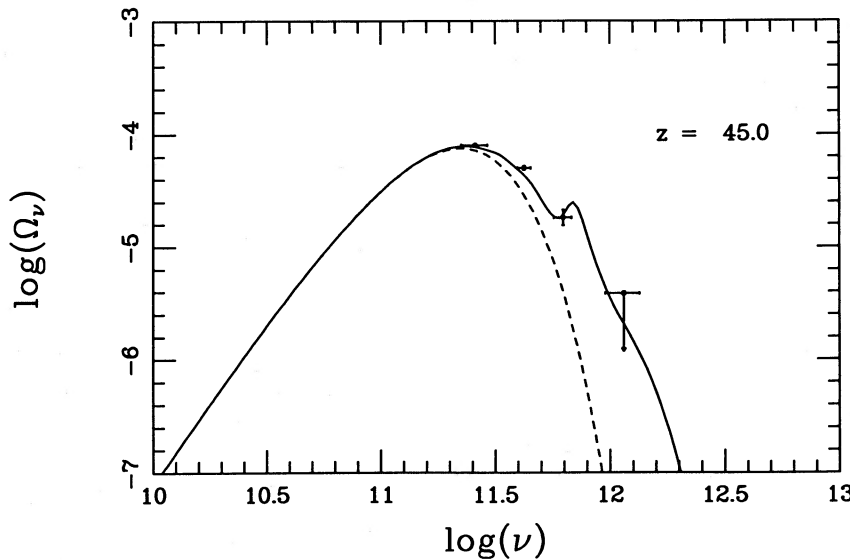


FIG. 3.—Dust distortion model at formation redshift $z = 45$. The original cosmic microwave background is shown as the dashed line; the total background is shown as a solid line and includes the contribution from a dust distortion model with $\Omega_* = 0.225$ and $\Omega_D = 1.5 \times 10^{-6}$.

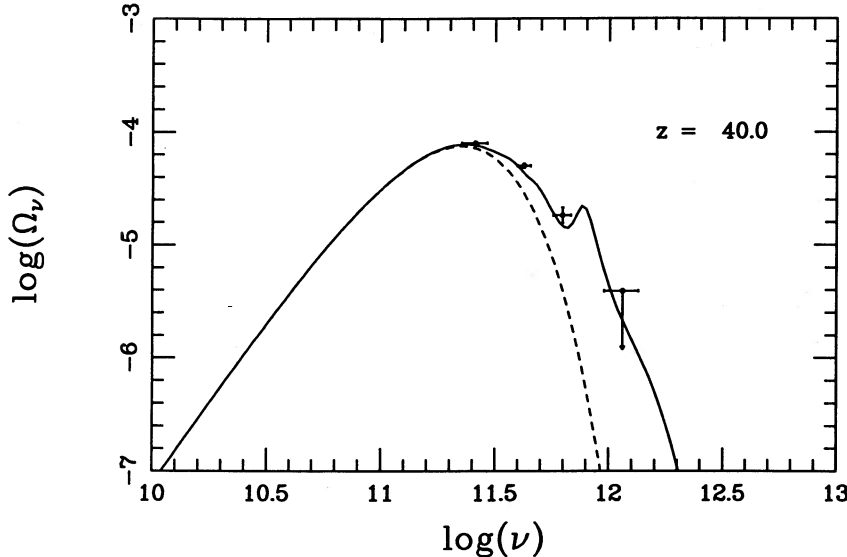


FIG. 4.—Dust distortion model at formation redshift $z = 40$. The original cosmic microwave background is shown as the dashed line; the total background is shown as a solid line and includes the contribution from a dust distortion model with $\Omega_* = 0.200$ and $\Omega_D = 2.0 \times 10^{-6}$.

Metallicity considerations may place further constraints on the allowed range of acceptable redshifts. If the dust grains become well mixed with the gas in regions that eventually form galaxies (and hence globular clusters and other Population II stars), the resulting metallicity will be given by $Z \approx \Omega_D/\Omega_b$. For $\Omega_b = 0.20$, the metallicity will be in the range $5 \times 10^{-4} \geq Z \geq 1.0 \times 10^{-5}$ for formation redshifts in the range $25 \leq z \leq 40$ (see Table 1). The observed metallicity for Population II objects (i.e., field stars and globular clusters) in our Galaxy follows a distribution with a reasonably well defined peak at approximately $Z = 5 \times 10^{-4}$ (see Laird *et al.* 1988). If this value is representative of the pregalactic metallicity, our range of allowed formation redshifts is not seriously reduced. On the other hand, a few stars have been observed with metallicities as low as $Z = 10^{-5}$ (see Laird *et al.* 1988 for the details of the metallicity distribution). If this smaller value

of Z were representative of the first Population II objects, a conflict would arise with the required values of Ω_D and successful dust distortion models would be restricted to a smaller region of parameter space (such as larger redshift models or smaller Ω_0). In any case, the metallicity of the first Population II objects is still controversial and many models of chemical evolution in galaxies require some initial enrichment (see Bond 1981; Hills 1982; Tarbet and Rowan-Robinson 1982). It is also possible that the dust grains are not well mixed with the gas that forms Population II objects and hence these metallicity constraints do not apply.

The preceding sequence of models was presented with fixed cosmological parameters; we will now show the effects of varying these parameters. In Figure 9, we illustrate the dependence on Ω_0 (since all quantities in the problem scale approximately as $\Omega_0 h_{50}^{-2}$ for $\Omega_0 z \gg 1$, this figure effectively illustrates

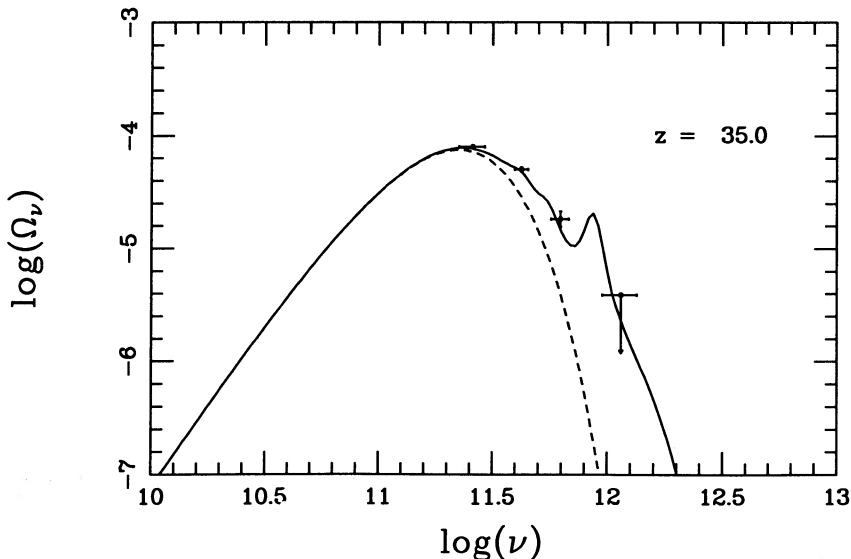


FIG. 5.—Dust distortion model at formation redshift $z = 35$. The original cosmic microwave background is shown as the dashed line; the total background is shown as a solid line and includes the contribution from a dust distortion model with $\Omega_* = 0.175$ and $\Omega_D = 5.0 \times 10^{-6}$.

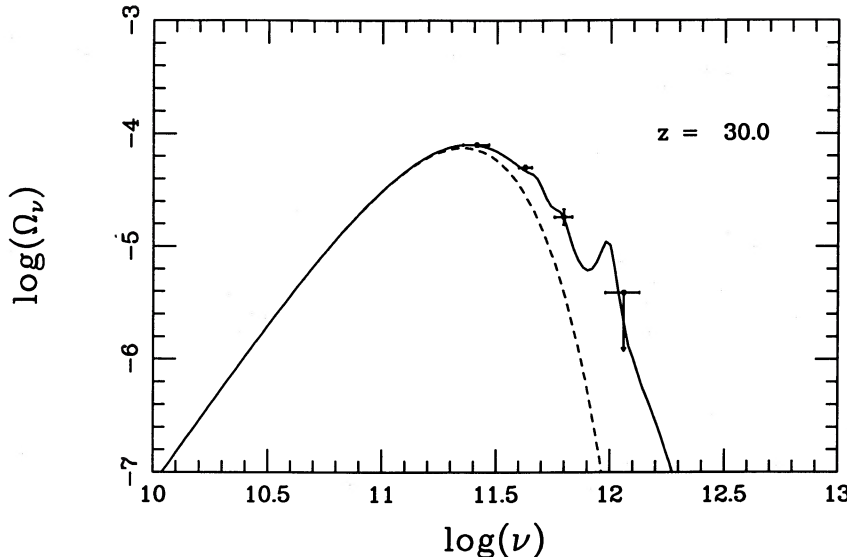


FIG. 6.—Dust distortion model at formation redshift $z = 30$. The original cosmic microwave background is shown as the dashed line; the total background is shown as a solid line and includes the contribution from a dust distortion model with $\Omega_* = 0.150$ and $\Omega_D = 7.0 \times 10^{-5}$.

the dependence on H_0 as well). For a smaller total energy density Ω_0 , the expansion rate decreases, and there is more path length (and hence more optical depth) for a given redshift of dust formation. Hence, a smaller value of Ω_D is adequate to produce the required optical depth. We can thus introduce dust at a lower redshift without violating the upper limit on the cosmic dust abundance and use a correspondingly lower value of Ω_* . For example, in Figure 9 we have taken $\Omega_0 = 0.1$, $\Omega_* = 0.08$, $\Omega_D = 10^{-4}$, and $z = 20$. We have considered this particular case to show that models with lower values of Ω_* can work without violating the dust abundance constraint.

The remaining cosmological parameter is the temperature T_0 of the (original) cosmic microwave background at the present epoch. However, the value of T_0 is tightly constrained by measurements on the long-wavelength side of the spectrum: $T_0 = 2.74 \pm 0.016$ K is the weighted mean of all of the mea-

surements performed to date (see Kogut *et al.* 1988; Johnson and Wilkinson 1987). Since the value of T_0 can vary by at most 0.6% (1.2%) at the 1σ (2σ) level, varying T_0 can produce at most a 2.4% (5%) change in the total energy of the microwave background and will not greatly affect the models of dust distortions presented in this paper. By assuming the largest possible value of T_0 , we could reduce the required amount of energy in the excess and thereby reduce the required values of Ω_* , but our basic conclusions would remain the same.

V. COMPTON DISTORTIONS

Free electrons in the universe can interact with the cosmic microwave background through Compton scattering. If a substantial amount of energy is released in the universe after the epoch of recombination, the temperature of the electrons T_e

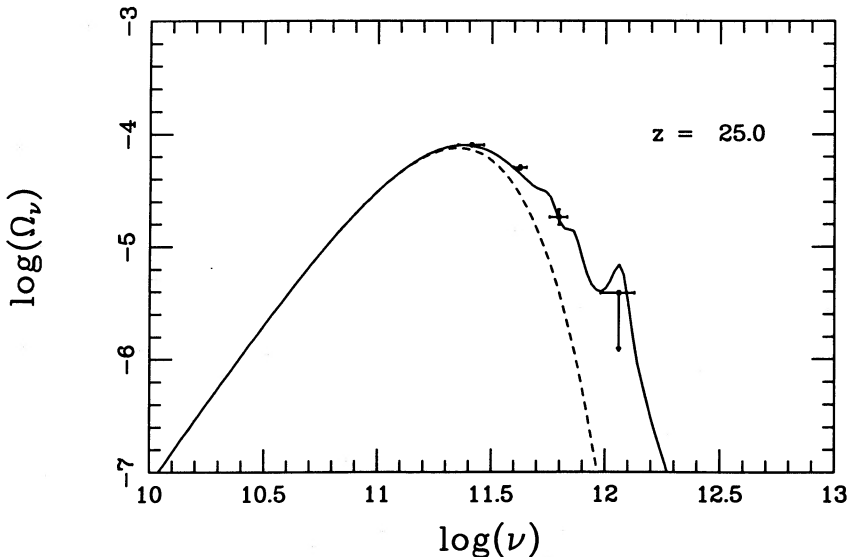


FIG. 7.—Dust distortion model at formation redshift $z = 25$. The original cosmic microwave background is shown as the dashed line; the total background is shown as a solid line and includes the contribution from a dust distortion model with $\Omega_* = 0.125$ and $\Omega_D = 10^{-4}$.

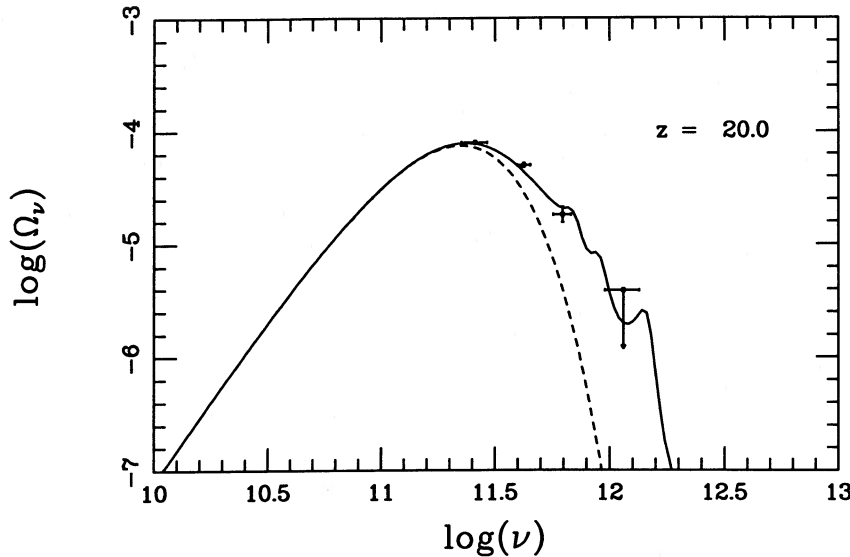


FIG. 8.—Dust distortion model at formation redshift $z = 20$. The original cosmic microwave background is shown as the dashed line; the total background is shown as a solid line and includes the contribution from a dust distortion model with $\Omega_* = 0.100$ and $\Omega_D = 2.0 \times 10^{-4}$.

can be raised above the temperature of the radiation T_{CMB} and Compton scattering can produce spectral distortions of the CMB. Under a wide range of physical conditions (as long as the electrons remain nonrelativistic—see Sunyaev and Zel'dovich 1980) the resulting spectrum of the radiation can be described by a single parameter y :

$$y \equiv \int_{z_1}^{z_2} \frac{k(T_e - T_{\text{CMB}})}{m_e c^2} \sigma_T n_e(z) c \frac{dt}{dz} dz, \quad (6)$$

where $\sigma_T = 8\pi/3(e^2/mc^2)^2$ is the Thompson cross section and n_e is the number density of electrons. In the limit $y \ll 1$ (which must apply to the observed distortion as we show below), the size of the distortion y is simply related to the amount of

injected energy ΔE

$$y = \frac{1}{4} \frac{\Delta E}{E_{\text{CMB}}},$$

where E_{CMB} is the initial energy of the cosmic microwave background. Furthermore, in the limit that $T_e \gg T_{\text{CMB}}$, the resulting radiation spectrum also has a simple form which can be written in terms of the radiation temperature as

$$\frac{\Delta T}{T} = y \left[x \left(\frac{e^x + 1}{e^x - 1} \right) - 4 \right], \quad (7)$$

where $x = h\nu/\kappa T_{\text{CMB}}$. At the present epoch (where $T_{\text{CMB}} = T_0$), the spectrum is thus completely specified by the two param-

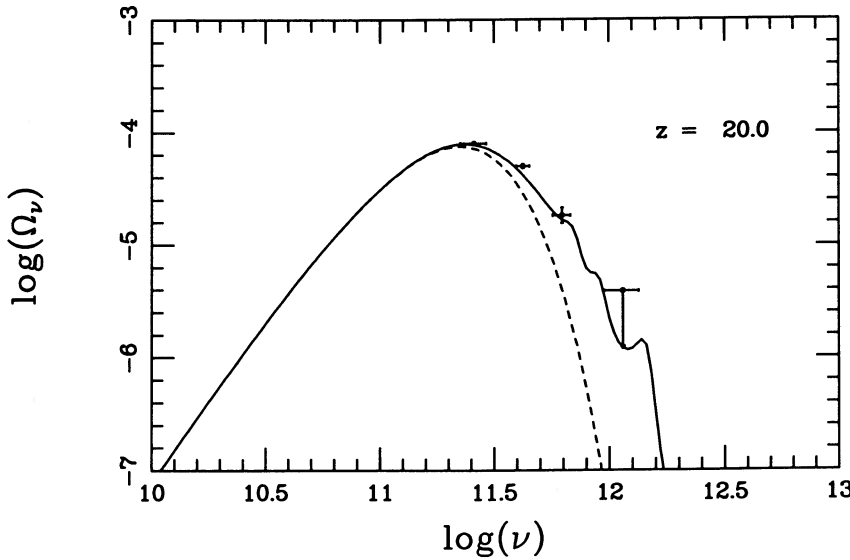


FIG. 9.—Dust distortion model for an open universe with $\Omega_0 = 0.1$ and a formation redshift $z = 20$. The original cosmic microwave background is shown as the dashed line; the total background is shown as a solid line and includes the contribution from a dust distortion model with $\Omega_* = 0.08$ and $\Omega_D = 10^{-4}$ (compare with Fig. 8).

eters T_0 and y . Notice, however, that since the scattering process adds energy to the short-wavelength side of the spectrum at the expense of the long-wavelength side, the observed temperature at long wavelengths T_{RJ} does not correspond to the unperturbed temperature T_0 as in the case of dust distortions. Instead, the two temperatures are related through $T_{RJ} = T_0(1 - 2y)$.

Hayakawa *et al.* (1987) have shown that the parameters $y = 0.028$ and $T_0 = 2.75$ K are consistent with the excess emission detected by Matsumoto *et al.* (1988). They argue that the resulting predicted temperature at long wavelengths ($T_{RJ} = 2.60$) is far below the observed weighted average at long wavelengths ($T = 2.74 \pm 0.016$; see Kogut *et al.* 1988) and thereby question the possibility of Compton distortions. However, this result was obtained under the assumption that the observed submillimeter excess is accurate to 1σ . If, on the other hand, we consider 2σ errors (assuming the uncertainty in the excess is at least this great) and then plot the allowed regions in the $y - T_0$ plane for each of the three channels of Matsumoto *et al.* (1988) and for the weighted average of the existing long wavelength measurements, we find a small region of parameter space consistent with all of the measurements (see Fig. 10). This region is also consistent with the observed upper limit in the fourth channel. The center of the allowed region corresponds to the values $y = 0.0167$ and $T_0 = 2.81$ K.

If the errors of the CMB measurements strictly followed Gaussian statistics, the probability of having all the measurements off by 2σ would be rather small. However, the measurement errors are likely to be dominated by systematic effects and hence the possibility of Compton y -distortions remains viable.

However, if Compton y -distortions are the explanation of the observed submillimeter excess, then an energy source is required to heat the electrons to a high-temperature $T_e \gg T_{CMB}$ (see Lacey and Field 1989 for a more detailed discussion of the energetic requirements). The energetic requirements are large

and most conventional sources (e.g., stars and supernovae) are ruled out (Lacey and Field 1989). Possible energy sources for Comptonization include decaying particles (Fukugita 1988; Field and Walker 1989 point out that there will be an over-production of UV photons), superconducting cosmic strings (Ostriker and Thompson 1987), and a decaying vacuum energy. In a previous paper outlining the history of the universe in the presence of a decaying vacuum energy (Freese *et al.* 1987), it was shown that a vacuum decaying to radiation with a non-Planckian spectrum (between redshifts of $z_i \sim 5 \times 10^4$ and $z_f \sim 10^3$) gives rise to y -distortions of the size

$$y = x \ln \left(\frac{z_i}{z_f} \right),$$

where $x \equiv \rho_{vac}/\rho_c$ is the ratio of vacuum energy density to the critical density. Hence $x \sim 0.0043$ can produce the requisite $y = 0.0167$ of the observed CMB (see also Bartlett and Silk 1989 for a discussion of y -distortions from decaying vacuum energy). However, μ -distortions are generated by radiation produced at an earlier epoch (Freese *et al.* 1987) and consistency with observations of μ -distortions probably forces x to be too small to explain the observed excess.

VI. DISCUSSION

The results of the preceding sections show that the shape of the observed spectral distortion of the CMB can be produced by both cosmic dust and by nonrelativistic Compton scattering. In the dust scenario, a significant amount of dust and an early generation of stars must be introduced into the universe at redshifts of $20 \leq z \leq 40$; however, we stress again that the model is consistent with existing cosmological constraints. Once the physical characteristics of the universe are set by observations independent of the observed submillimeter excess, the remaining parameters are the dust abundance Ω_D , the source abundance Ω_* , and the formation redshift z . Since

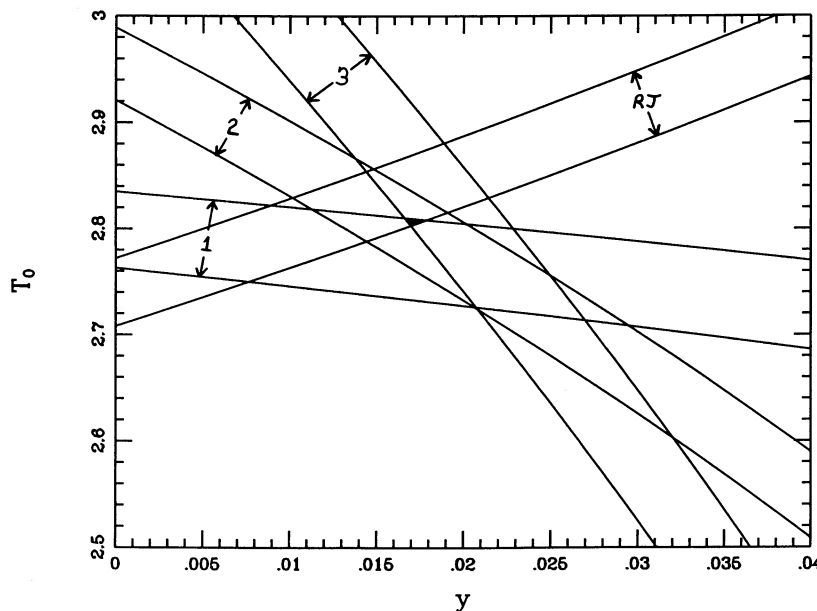


FIG. 10.—Allowed region in the $y - T_0$ plane for Compton y -distortions. Each individual band is the allowed region for a single datum, assuming an error of 2σ . The bands labeled 1–3 correspond to the first three channels of the Matsumoto *et al.* experiment (1988) and the band labeled RJ corresponds to the weighted mean of all of the long-wavelength experiments performed to date (see Kogut *et al.* 1988). The shaded region near the center (i.e., the intersection) is the allowed region in the plane and implies values of $T_0 = 2.81$ and $y = 0.0167$.

two of these parameters are related through energetic considerations (see § III), the number of parameters for our sequence of models is limited to two. One potential diagnostic in this scenario is the silicate feature, which appears in emission and gets redshifted into the submillimeter excess. If future experiments with narrow-band filters detect such features in the submillimeter excess, then the case for dust distortions will be greatly enhanced.

Our calculations have used dust opacities consistent with the observed extinction curve in our Galaxy. It is possible that pregalactic dust has different optical properties and that the required values of Ω_D are smaller than our calculations indicate. However, it has been shown (see Draine and Shapiro 1989) that even if the dust grains had the optimum properties (that do not violate the laws of physics), the required amount of dust (i.e., Ω_D) is only smaller by approximately a factor of 3.

One possible concern is that nearly all of the available baryons in the universe must be processed into VMOs in order to produce the required energy, i.e., the required values of Ω_* (see Table 1) are comparable to the maximum allowed values of Ω_b from BBN. Although the required value of Ω_* can be reduced somewhat by more judicious parameter choices (e.g., assuming the largest possible value of T_0), a rather high efficiency of VMO production is still necessary. Although there is no *a priori* theory which demands the production of VMOs, there is no way (at present) to rule out their existence (see Carr, Bond, and Arnett 1984 and McDowell 1986 for further discussion of this issue). In particular, in a theory with linear perturbation growth, the anisotropy produced in the CMB from the primordial perturbations that produced the VMOs will have an angular scale $\theta \ll 1''$; hence any such anisotropy will be unobservable with present technology. For a discussion of the formation of stars at such early redshifts, see Bond, Carr,

and Arnett (1986); in fact, success of dust scenarios may indicate the existence of new interesting physics such as alternatives to linear perturbation growth (e.g., the work of Hill, Schramm, and Fry 1988).

In any case, the general model of dust distortions does not require that the energy source be VMOs—any sufficiently energetic source will suffice. For example, other authors (see Fukugita 1988; Field and Walker 1989) have considered the possibility of decaying particles producing an ultraviolet radiation field which in turn heats electrons and leads to Compton distortions. Decaying particles could also be the source of UV radiation in our dust distortion models, provided that the required amount of energy is produced. (In a model in which decaying particles provide energy for Comptonization, UV radiation is overproduced; in a dust model with decaying particles, however, dust absorption removes the UV background problem.)

In conclusion, we feel that the cosmic dust distortion mechanism is a viable explanation for the observed excess radiation at submillimeter wavelengths. The models presented here remain consistent with existing astrophysical constraints and require nothing more exotic than dust and stars.

We would especially like to thank G. Field for his encouragement and advice. We are grateful to G. Bernstein, A. Cameron, B. Draine, A. Lange, D. Latham, G. Rybicki, A. Stebbins, B. Wang, E. Wright, and T. Walker for useful discussions during the preparation of this paper. We also acknowledge L. Lellouch for preliminary calculations pertaining to this work. In addition, we thank the Institute for Theoretical Physics in Santa Barbara for hospitality during the writing of this manuscript.

APPENDIX

NUMERICAL FORMULATION

For the numerical treatment, it is convenient to work in terms of a flux which is invariant with redshift,

$$F_{v_0} \equiv \frac{v I_v}{(1+z)^4}, \quad (\text{A1})$$

where $v_0 = v/(1+z)$. For a given dust temperature distribution $T_D(z)$, the equation of transfer in the absence of source terms then takes the form,

$$\frac{\partial F_{v_0}(t)}{\partial t} = \Omega_D \rho_C c \kappa_v \left\{ F_{v_0}^{(\text{eq})} \left[\frac{T_D(z)}{(1+z)} \right] - F_{v_0} \right\}, \quad (\text{A2})$$

where

$$F_v^{(\text{eq})}[T] = \frac{15a(h/k)^4}{\pi^4 \rho_C c^2} \frac{v^4}{\exp(hv/kT) - 1} \quad (\text{A3})$$

is the equilibrium radiation density per logarithmic frequency interval (corresponding to the Planck function). Notice that the fluxes are evaluated at the present day frequency v_0 , but the opacity κ_v must be evaluated at the instantaneous frequency $v = v_0(1+z)$ of the photon. In terms of the optical depth,

$$\tau_{v_0}(z_D, z) = \int_z^{z_D} \Omega_D \rho_C \kappa_v c (1+z')^3 \frac{dt}{dz'} dz', \quad (\text{A4})$$

the equation of transfer (A2) can be written

$$\frac{\partial F_{v_0}(z)}{\partial \tau_{v_0}(z)} = F_{v_0}^{(\text{eq})} \left[\frac{T_D(z)}{(1+z)} \right] - F_{v_0}, \quad (\text{A5})$$

which is the form actually used in the numerical procedure. The equation of radiative balance (which determines the temperature distribution) can be written in terms of invariant quantities as

$$\int_0^\infty F_{v_0}^{(eq)} \left[\frac{T_D(z)}{1+z} \right] \kappa_v d(\ln v_0) = \int_0^\infty F_{v_0}(z) \kappa_v d(\ln v_0), \quad (A6)$$

which is equivalent to equation (3) in the text.

Equations (A4)–(A6) are solved self-consistently to find the dust temperature at each epoch. The step size for each incremental epoch is chosen so that $\Delta\tau_v < 0.1$ at any frequency where the input spectral flux is more than one percent of the peak flux. The dust absorption and emission are then calculated assuming that the temperature is constant over the duration of the step.

Notice that in our model the radiative transfer integration is over time rather than over a spatial path as in most problems. At each epoch, the universe is assumed to be uniform and a one-zone model is calculated: there is of course no “back-reaction” to earlier epochs, so an iterative solution is not required. This feature makes the problem much easier to solve than an otherwise similar problem in a spatial dimension.

REFERENCES

- Adams, F. C., and Shu, F. H. 1986, *Ap. J.*, **308**, 836.
 Alcock, C. R., Fuller, G. M., and Mathews, G. J. 1987, *Ap. J.*, **320**, 439.
 Applegate, J. H., Hogan, C. T., and Scherrer, R. J. 1987, *Phys. Rev. D*, **35**, 1151.
 Bartlett, J., and Silk, J. 1989, in preparation.
 Bernstein, G. M., Fischer, M. L., Richards, P. L., Peterson, J. B., and Timusk, T. 1989, *Ap. J. (Letters)*, submitted.
 Bond, J. R. 1981, *Ap. J.*, **248**, 606.
 Bond, J. R., Carr, B. J., and Arnett, W. D. 1984, *Ap. J.*, **280**, 825.
 Bond, J. R., Carr, B. J., and Hogan, C. 1986, *Ap. J.*, **306**, 428.
 Carr, B. J., Bond, J. R., and Arnett, W. D. 1984, *Ap. J.*, **277**, 445.
 Draine, B. T., and Lee, H. M. 1984, *Ap. J.*, **285**, 89.
 Draine, B. T., and Shapiro, P. 1989, *Ap. J. (Letters)*, submitted.
 Field, G. B., and Walker, T. P. 1989, preprint.
 Freese, K., Adams, F. C., Frieman, J. A., and Mottola, E. 1987, *Nuc. Phys. B*, **287**, 797.
 Fukugita, M. 1988, *Phys. Rev. Letters*, **61**, 1046.
 Fuller, G. M., Mathews, G. J., and Alcock, C. R. 1987, *Phys. Rev. D*, submitted.
 Hayakawa, S., Matsumoto, T., Matsuo, H., Murakami, H., Sato, S., Lange, A. E., and Richards, P. L. 1987, *Pub. Astr. Soc. Japan*, **39**, 941.
 Hills, J. G. 1982, *Ap. J. (Letters)*, **258**, L67.
 Hill, C. T., Schramm, D. N., and Fry, J. N. 1988, preprint.
 Hogan, C. J., and Bond, J. R. 1988, in *The Post-Recombination Universe*, ed. N. Kaiser and A. Lasenby (Dordrecht: Kluwer), p. 141.
 Johnson, D. G., and Wilkinson, D. T. 1987, *Ap. J. (Letters)*, **313**, L1.
 Kawano, L., Schramm, D. N., and Steigman, G. 1988, *Ap. J.*, **327**, 750.
 Kogut, A., et al. 1988, *Ap. J.*, **325**, 1.
 Lacey, C. G., and Field, G. B. 1989, *Ap. J. (Letters)*, in press.
 Laird, J. B., Rupen, M. P., Carney, B. W., and Latham, D. W. 1988, *A.J.*, **96**, 1908.
 Matsumoto, T., Hayakawa, S., Matsuo, H., Murakami, H., Sato, S., Lange, A. E., and Richards, P. L. 1988, *Ap. J.*, **329**, 567.
 McDowell, J. C. 1986, *M.N.R.A.S.*, **223**, 763.
 McDowell, J. C., Elvis, M., Wilkes, B. J., Bechtold, J., Green, R. F., Oey, M. S., and Polomski, E. F. 1989, in preparation.
 Negroponte, J. 1986, *M.N.R.A.S.*, **222**, 19.
 Negroponte, J., Rowan-Robinson, M., and Silk, J. 1981, *Ap. J.*, **248**, 58.
 Ostriker, J. P., and Thompson, C. 1987, *Ap. J. (Letters)*, **323**, L97.
 Penzias, A. A., and Wilson, R. W. 1965, *Ap. J.*, **142**, 419.
 Puget, J. L., and Heyvaerts, J. 1980, *Astr. Ap.*, **83**, 10.
 Rowan-Robinson, M., Negroponte, J., and Silk, J. 1979, *Nature*, **281**, 635.
 Sale, K. E., and Mathews, G. J. 1986, *Ap. J. (Letters)*, **309**, L1.
 Savage, B. D., and Mathis, J. S. 1979, *Ann. Rev. Astr. Ap.*, **17**, 73.
 Shu, F. H., Adams, F. C., and Lizano, S. 1987, in *Fermi School Lectures*, in *Interstellar Dust and Related Topics*, ed. S. Aiello.
 Sunyaev, R. A., and Zel'dovich, Y. B. 1980, *Ann. Rev. Astr. Ap.*, **18**, 537.
 Tarbet, P. W., and Rowan-Robinson, M. 1982, *Nature*, **298**, 711.
 Woody, D. P., and Richards, P. L. 1981, *Ap. J.*, **248**, 18.
 Wright, E. L. 1981, *Ap. J.*, **250**, 1.
 Yang, J., Turner, M. S., Steigman, G., Schramm, D. N., and Olive, K. 1984, *Ap. J.*, **281**, 493.

Note added in proof.—After the completion of this paper, we learned that E. Wright has done similar calculations in unpublished work; his results are in agreement with ours. In addition, related work has been done recently by Bond, Carr, and Hogan (*Ap. J.*, submitted [1989]). This work has been supported in part by Sloan Foundation grant No. 26722 (K. F.) and by NASA grant NAGW-1320 (J. L.) at MIT.

FRED C. ADAMS and JONATHAN C. McDOWELL: Harvard-Smithsonian Center for Astrophysics, 60 Garden Street, Cambridge, MA 02138

KATHERINE FREESE and JANNA LEVIN: Physics Department, Massachusetts Institute of Technology, Cambridge, MA 02139